Scientific Research Publishing

Aplication of *in Vivo* Confocal Microscopy in Ophtalmology—Overview

Ralitsa Kermedchieva*, **Marieta Konareva-Kostianeva, Marin Atanassov, Vesela Mitkova-Hristova, Nina Stoyanova**

Faculty of Medicine, Medical University of Plovdiv, Plovdiv, Bulgaria
Email: *rkermedchieva@yahoo.com

Abstract

Confocal microscopy is a method which has been increasingly used over the last decade in the study of the anterior ocular surface. The method allows testing and *in vivo* high resolution imaging of the structures of the anterior eye segment, at a cellular level, which is close to the histological examination of tissues. The data provided by this method allow for a better understanding of both the functional and pathological processes occurring in the anterior ocular surface not only for scientific purposes but also in clinical practice. The aim of the present work is to summarize the current knowledge and applications of confocal microscopy of the anterior ocular surface.

Keywords

Confocal Microscopy, Ocular Surface, Cornea, Corneal Dystrophies, Keratitis, Trabeculectomy

1. Introduction

In vivo confocal microscopy is a non-invasive method, which provides high resolution tissue images at a cellular level in real time, permitting the quantitative, qualitative and morphological analyses of a living tissue These capabilities can be employed to image structures of ocular surface in the eye, *in vivo*, both for research and for the diagnosis and treatment of human disease [1]-[7]. The ocular surface is composed of cornea, eyelid and the bulbous conjunctiva, as well as the eyelids [8]. The tear film plays an important role in maintaining the homeostasis of this system.

The method provides information and an opportunity for a better understanding of the ongoing processes in these structures, in depth.

Principle of Work

Confocal microscopy is a non-invasive imaging method that provides significantly higher image contrast than conventional light microscopy. The method of imaging with a confocal microscope is fundamentally different from that with a conventional light microscope, where the whole specimen is illuminated by a light source and the image can be observed directly by the eye [9].

With confocal microscopes, an aperture is used, situated on the image plane, and restricting the flow of diffuse light from the background. This allows for a series of two-dimensional images to be obtained at different depths of the focal plane in the examined specimen (the so-called optical section of the specimen in depth), with the possibility of subsequent construction of a three-dimensional image of the specimen.

The confocal approach provides magnification of the specimen, both laterally and axially, eliminating the "out of focus" fluorescence, which makes it a valuable and popular method [9].

The principle of confocal imaging, patented in 1957 by Marvin Minsky [9] [10], was designed to overcome certain limitations of conventional light microscopes, where the whole specimen is evenly illuminated by the light source, due to which the quality of images is distorted by the background unfocused part of the specimen.

In contrast, with confocal microscopes the light beam emanates from a single point, the aperture being located in front of the detector, eliminating the signal outside the focus—"confocal" derives from this configuration. Since it detects only light obtained from fluorescence close to the focal plane, the optical resolution of the image, especially in the depth of the specimen, is considerably better than that of conventional light microscopes.

One of the most widely used laser scanning confocal microscopes was designed by White, Amos, Durbin and Fordham [11] to image specific macromolecules in embryos [9]. This and some other microscopes developed at the time were the forerunners of modern microscopes, which are available to biomedical researchers.

Over the last decade, the method has become increasingly popular and widely applicable in many fields of medicine and biology. The advantages of confocal microscopy are hidden in the extremely high quality images, which provide information in detail about the microstructure of the examined specimen. In addition, the method has the potential to be used in many areas of biomedicine.

Master and Thaer described the application of a slit scanning confocal microscope, which performs a unique real-time video image of a live human cornea [8] [12] [13].

There are three types of CFM according to the type of illumination used:

1) Tandem Scanning Confocal Microscopy (TSCM), which is based on a modified technology with a Nipkow disc—a metal disc with multiple holes with a size of 30 microns, which rotates at a high speed. It was first introduced by

Canaugh *et al.* in 1989. They demonstrated a confocal image of epithelium, basal membrane, Bowman's membrane, stromal nerves, Descemet's membrane and endothelium of a live human cornea [14] [15]. In 1994, James Hill received a patent for the first tandem scanning confocal microscope.

2) Slit Scanning Confocal Microscopy (SSCM) with improved light output and faster image acquisition, but at the expense of axial resolution [14] [16]. Master and Thaer described the application of a slit scanning confocal microscope, which performed a unique real-time video image of a live human cornea [8] [12] [13]. Confoscan 4 (Nidek technologies Co., Ltd, Tokyo, Japan) is currently available on the market of this type [8].

3) Laser scanning confocal microscopy (LSCM)—it uses a coherent light source of high intensity, and the laser beam is scanned onto the back of the lens, using a set of galvanometric mirrors for scanning [12] [17] [18]. The method is fast and creates a high resolution image of 384 × 384 DPI in a 400 micron field. It provides higher contrast than TSCM and SSCM and has a better axial resolution of 4 microns compared to TSCM—8 - 25 microns, and SSCM—9 - 12 microns [14] [16].

Heidelberg Retina Tomograph (HRT) (Heidelberg Engineering, Heidelberg, Germany) is a well-developed, *in vivo* positioned confocal system. HRT uses a 670 μm diode laser and is designed to image and evaluate the optic nerve head in glaucoma. Steve and colleagues (University of Rostock, Germany) modified HRT with a lens system in the "Rostock Cornea Module"—a laser scanning high-resolution confocal microscope for the visualization of the anterior ocular segment, which allows the photographing of thin layers (optical slices) of the cornea [8] [19].

The main advantage of LSCM is precisely the ability to perform a series of thin high resolution optical slices *in vivo* for a short time [8]. This gives a precise and accurate assessment of the test specimen. Over the last decade, the method has gained wide popularity in the study of diseases of the ocular surface in live eyes.

Confocal microscopy allows for detailed examination and evaluation, at a cellular level, of the central and peripheral cornea, bulbar and eyelid conjunctiva, limbus, tear film and keratitis, after surgery of the anterior ocular segment.

2. *In Vivo* Laser Scanning Confocal Microscopy (LSCM) Characteristics of the Anterior Ocular Surface, in the Norm

2.1. Conjunctiva

The palpebral conjunctiva is characterized by the presence of the crypts of Henle. It is composed of stratified squamous non-keratinizing epithelium with cell dimensions of 10 - 15 μm, organized in 6 - 7 layers, followed by the conjunctival stroma, consisting of connective fibrils, blood vessels and accumulated hyperreflective cells—most likely lymphocytes and plasma cells.

Cysts with hyperreflective cells are sometimes found in the stroma. Relatively large cells (about 25 μm) are detected, supposed to be goblet cells. Fine capillaries up to 20 μm in size with blood cell elements in the lumen of the vessel—small hyperreflective structures—are found in the stromal layer. The vessels close to the eyelash margin have a larger diameter, and the vessel wall can be observed in an image in the oblique diameter.

The eyelash margin is represented by a layer of epithelial cells and the secretory ducts of the Meibomian glands, in which lipid accumulations can be detected [20].

The bulbar conjunctiva is thinner than the palpebral conjunctiva. It is characterized by smaller epithelial cells (about 10 μm) with hyperreflective inclusions (lymphocytes and plasma cells), as well as fewer goblet cells, compared to the palpebral and fornix conjunctiva. The palisades of Vogt are clearly visible in the limbal area.

2.2. Cornea

Confocal microscopy allows *in vivo* layer-by-layer images of the cornea, which are similar to a histological section (Figure 1).

Epithelial layer (*Corneal epithelium*): it is composed of 5 - 6 layers of epithelial cells, functionally and morphologically divided into 3 zones:

- Superficial cells: they have a polygonal shape, 40 - 50 μm in diameter and about 5 μm thick (Masters and Thaer 1995; Tomii *et al.* 1994) [2] [21]. They are characterized by a small reflective nucleus surrounded by a hyporeflective ring and dark cytoplasm. They have well-defined boundaries. Approximately one-seventh of these cells are lost through desquamation within 24 hours, changing their optical characteristics [22]. Variations in cytoplasmic reflectivity are observed depending on the stage of desquamation—increased cytoplasmic reflectivity with a clearly distinguishable nucleus with a dark halo [8] [21]. The density of the cells varies from 850 cells/sq·mm to 1200 cells/sq·mm in the central and peripheral part of the cornea [2] [20] [22] [23].
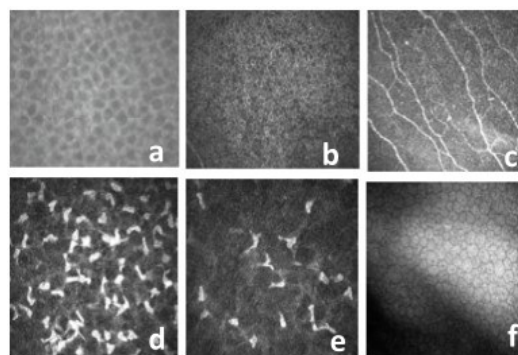

Figure 1. Representative *in vivo* confocal images of normal human cornea (Bar represents 50 μm): (a) wing and (b) basal epithelial cells; (c) subepithelial nerve plexus; (d) anterior stroma; (e) posterior stroma; (f) endothelium.

- Wing cells: they have a polygonal shape and well-defined borders with a mosaic appearance (**Figure 1(a)**). They range in size: the more superficially positioned ones are 50 μm in diameter, whereas the deeper ones are 20 μm. The density varies from 5000 cells/sq·mm in the central part of the cornea up to 5500 cells/sq·mm. in the periphery [8].
- Basal cells: they have an elongated shape, a small diameter of 8 - 10 μm and a height of 20 μm. They are characterized by clearly distinguishable borders and a nucleus hard to differentiate (**Figure 1(b)**). The density in the central cornea varies from 6000 cells/sq·mm up to 9000 cells/sq·mm, and 10,000 cells./sq.mm in the periphery [2] [8] [20] [23] [24].

Bowman's membrane (*anterior limiting membrane*): an amorphous membrane located just below the basal epithelial cells, with a thickness of approximately 10 μm. It is composed of collagen fibrils and contains unmyelinated nerve fibers from the subepithelial nerve plexus [20] [21].

Corneal nerves. The cornea is the structure of highest sensitivity in the human body. This is due to the large number of nerve fibers running through it. This extensive innervation affects the integrity of the corneal epithelium and the healing of corneal injuries [20] [25]. The visualization and examination of these nerve fibers is possible with confocal microscopy.

Nerve fibers are sensory, deriving from the ophthalmic nerve and the terminal branches of the trigeminal nerve. They have no myelin sheaths, their thickness varying from 2 μm to 10 μm. Nerve fibers enter from the peripheral part of the cornea into the anterior and middle parts of the stroma. They run parallel to the corneal surface, moving along radially before making a sharp turn at 90 degrees towards Bowman's membrane [20] [26].

The nerve fibers reach the corneal apex mainly along the meridians at 6 - 12 h, 5 - 11 h or 7 - 1 h and keep a course predominantly in an upward-downward direction (12 - 6 h); in the other areas, they are oriented in a nasal-temporal direction [26].

In the anterior parts of the stroma, just before Bowman's membrane, the nerve fibers divide in three directions. Some of them branch without penetrating Bowman's membrane, forming **the Subepithelial Plexus (SEP)** (**Figure 1(c)**). Thin nerve fibers of the SEP are characterized by fibers connected with anastomoses. The profile of these fibers is hyperreflective, and their tickness usually ranges from 4 to 8 μm [25] [26] [27] [28]. Others penetrate Bowman's membrane directly, following a perpendicular or slightly oblique course or form fine branches just before piercing the membrane. After passing through Bowman's membrane, they change their course to 90 degrees and run between the basal epithelial layer and the membrane towards the center of the cornea, forming **the Basal Epithelial Plexus** (**BEP**). They then form multiple branches in all directions along the corneal surface, where they end loosely or in the direction of the center of the cornea [20] [26] [27].

The nerve fibers from the basal epithelial plexus usually run parallel to each other, forming Y or T-branches.

Confocal microscopy images show the stromal nerve fibers as thick [8], almost always taut, highly reflective structures, often located near keratocytes, the deep stroma lacking nerve fibers.

The nerve fibers of the basal epithelial plexus are characterized by lower reflectivity, a predominantly granular structure and tortuous course. The thicker fibers branch out, reuniting after a certain distance to form a fiber of the same size. There are also many small nerve branches which form connections between long nerve fibers [20] [26] [27].

Corneal stroma: makes up about 90% of the volume of the cornea. It consists of three main components: cellular-keratocytes, amorphous substance (glycoproteins, glucose-aminoglycans—keratin sulfate and chondroitin sulfate) and nerve fibers. The nuclei of the keratocytes are highly reflective, in the shape of a "bean" in the anterior parts of the stroma (**Figure 1(d)**), and "egg-shaped" in the deep layers (**Figure 1(e)**). The other cell structures are not visible – they appear black. The density of keratocytes is higher in the anterior parts of the stroma. The nerve fibers in the stroma are larger in diameter than the subepithelial ones [8] and keep a rectilinear course.

Descemet's membrane. Posterior limiting lamina. This membrane is the basal membrane of endothelial cells. Its thickness varies from 6 μm to 10 μm. In a confocal image it is seen as a homogeneous acellular layer. Normally it cannot be imaged in young individuals. With the advancement in age, however, it is easier to image (Hollingsworth *et al*. 2001) [8] [21].

Corneal endothelium: a single layer of endothelial cells with a hexagonal or polygonal shape with dimensions: 4 - 6 μm thick and about 20 μm in diameter. In a CFM image they resemble a "honeycomb" mosaic with clear dark borders and hyperreflective cytoplasm, without polymegatism (variations in cell size) and pleomorphism (variations in the shape of the cell) (**Figure 1(f)**). The nucleus is rarely distinguished [8] [21]. The total number of endothelial cells in a healthy individual is approximately 500,000 cells. The density in the central cornea is 2500 - 3000 cells/sq·mm [8]. Their number decreases with age by approximately 0.6% per year (Efron *et al*. 2001; Joyce 2003), polymegatism being also on the rise (Efron *et al*. 2001) [21].

In patients with diabetes, edothelial damage increases (Inoue *et al*. 2002) and an increased incidence of polymegatism is established depending on when the disease started (Lee *et al*. 2006). A study by Roszkowska *et al*. in 1999 showed a reduced endothelial cell density by 5% in the type 2 diabetes group and 11% – in the type 1 diabetes group, compared to the control age group [21].

Limbal region: it is the boundary zone between the cornea and conjunctiva and the underlying sclera, which plays an important role in maintaining the integrity of the cornea. A border is formed between the corneal epithelium and the conjunctival epithelium, which consists of approximately 10 - 12 layers. Here the palisades of Vogt are found too [20]. It is assumed that it is in the palisades of Vogt that limbal stem cells are synthesized for the regeneration of the corneal epithelium [29] [30]. When CFM imaged, the epithelial cells of the conjunctiva

appear more highly reflective, with unclear borders and smaller in size; they have larger and brighter nuclei. In the border zone, epithelial cells are characterized by inhomogeneous reflectivity and variations in shape and size [20].

The palisades of Vogt are visualized as trabecular extensions in the conjunctival epithelium, located radially to the limbus. Their edges are well demarcated, especially in the deeper layers, at the end of which concentrations of hyporeflective cells are differentiated, supposed to secrete stem cells [20].

In the subepithelial space, near the limbus, there are blood vessels—limbal plexus.

3. *In Vivo* Laser Scanning Confocal Microscopy (LSCM) Characteristics in Anterior Ocular Surface Diseases

The ability of CFM to produce rapid *in vivo* layer-by-layer images of tissues, even with decreased corneal transparency, makes it an extremely valuable method in the diagnosis, follow-up and treatment of many pathological conditions of the anterior segment of the eye. It gives us a new understanding of the ongoing pathophysiological processes at a cellular level, enabling us to monitor and evaluate treatment.

3.1. Corneal Dystrophies

The most common classification of corneal dystrophies is anatomically based (IC3D classification of Corneal Dystrophies). The dystrophies are divided into groups, depending on the corneal layer affected.

In 2015, the IC3D classification of Corneal Dystrophies—Edition 2, was revised and published, the templates being updated, as a result of which the dystrophies are now divided into four major groups: epithelial and subepithelial, epithelial—stromal, stromal and endothelial [31].

Until recently, the clinical evaluation, diagnosis and differentiation of corneal dystrophies were based on biomicroscopy, but it was unable to provide information at a cellular level. It necessitated the performance of a biopsy, as well as genetic and histological examination, which are invasive and time-consuming methods [21].

On the other hand, CFM is a rapid non-invasive method which provides information at a cellular level *in vivo*, quickly finding a place in the diagnosis of corneal dystrophies [32].

Epithelial and subepithelial corneal dystrophies

Epithelial dystrophies are relatively more frequent compared to other varieties [12] [33] [34].

The most common among them is Epithelial Basement Membrane Dystrophy (EBMD) (map-dot-fingerprint), which manifests itself clinically with recurrent erosions in about 10% of the cases. What is observed are grayish linear opacities with sharp outlines (maps), optically empty or whitish dots and grayish fine lines (fingerprints) in the corneal epithelium. CFM visualizes highly reflective linear

tissue, located between the layers of the middle and basal epithelium. Highly reflective cysts with sizes between 10 - 400 μm are also differentiated. The basal epithelial cells around the abnormal basal membrane are larger in size, irregularly shaped, having highly reflective nuclei. Changes are detected in the subbasal nerve plexus, with a reduction in the number of long nerve fibers and their course [31] [32] [35] [36] [37] [38].

Meesmann Corneal Dystrophy (MECD) is an autosomal dominant disorder, characterized by the presence of numerous small cysts or vacuoles in the epithelial layer, also visible on biomoroscopy. CFM displays well-demarcated hyporeflective areas of the basal epithelial layer with a diameter of 40 - 150 μm, corresponding to the cysts, visible through biomicroscopy. The presence of hyperreflective material in the form of hyperreflective dots is visible between most hyporeflective zones [31] [32] [39] [40] [41].

With map-dot-fingerprint corneal dystrophy, CFM visualizes extensive cystic lesions without the presence of hyperreflective material, in contrast to Meesmann corneal dystrophy, where there is one [40].

Lisch Epithelial corneal dystrophy (LECD) is a rare condition, characterized by a highly reflective cytoplasm of the epithelial cells and a hyporeflective nucleus in well-defined areas, affecting all epithelial layers, involving the limbal area too.

Gelatinous Droplike Dystrophy (GDLD), where amyloid material is present in the subepithelial space, is characterized by disorganization in the architecture and change in the shape of epithelial cells. CFM shows extensive hyperreflective areas of accumulated amyloid between the epithelium and the anterior stroma, with nerve fiber interruptions in the subepithelial plexus. The posterior layers of the cornea are not affected [31] [32].

Epithelial—stromal corneal dystrophies

With its high image resolution, CFM makes it possible to identify and differentiate between Reis-Buckler Corneal Dystrophy (RBCD) and Thiel-Benke Corneal Dystrophy (TBCD), unlike biomicroscopy [12] [42] [43] [44]. Known as dystrophies type 1 and type 2, they affect Bowman's membrane. TBCD is with autosomal dominant inheritance, while with RBCD a mutation in the TGFBI gene has been established [32].

In both dystrophies there are deposits of hyperreflective material in the epithelium and Bowman's membrane. In TBCD the reflectivity is moderate; there are rounded borders and a concomitant dark halo (Figure 2), in contrast to RBCD, where the deposits have very high reflectivity, pronounced granulation and a lack of halo [43].

With RBCD, fine fusiform deposits can be observed in the anterior and rarely in the posterior parts of the stroma [31].

Lattice corneal dystrophy (LCD) is caused by the mutation of Arg124Cys and Leu527Arg in the TGFBI gene [45]. Through biomicroscopy, a multitude of fine fibers and radial particles in the stroma, corresponding to amyloid deposits, are
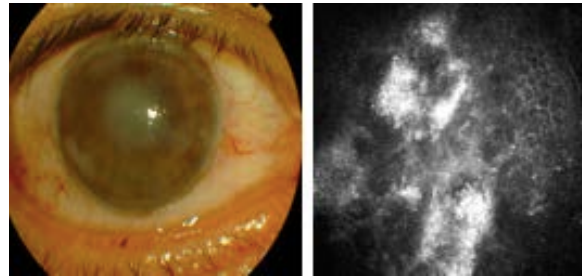
Figure 2. Thiel-Benke Corneal Dystrophy (TBCD). *In vivo* confocal microscopy image shows abnormal hyperreflective material with homogeneous reflectivity, round edges, and dark shadows within the basal epithelium.

observed. Kaufman *et al.* were the first to describe a case of primary corneal amyloidosis, demonstrating the high hyperreflectivity of the amyloid deposits with CFM [46]. Consequently, many studies established the presence of hyper-reflective extracellular punctate deposits in the basal epithelium layer [44] [47]. Linear filaments with different reflectivity and unclear borders, with thickness of up to 50 μm and a dimeter of 80 - 100 μm, are found in the stroma [44] [47] [48], (Figure 3). A reduction of the long nerve fibers is detected in the subbasal nerve plexus, which results in decreased corneal sensitivity, described in the case of lattice type 2 (familial amyloidosis) [32] [49].

Granular corneal dystrophy (GCD) is with autosomal dominant inheritance, caused by a mutation in the TGFBI gene. Hyaline deposits, involving the central corneal zone, are found in the corneal stroma and Bowman's membrane, leading to reduced corneal transparency [45]. CFM images show hyperreflective "snow-ball" or trapezoid-like deposits in the posterior epithelial layers and Bowman's membrane. The deposits in the stroma vary from 50 μm to 500 μm in diameter, the size decreasing in the deeper layers. The lesions are dense with well-defined borders against the surrounding normal stroma [32] [44].

Stromal corneal dystrophies

Macular Corneal Dystrophy (MCD) is characterized by the appearance of whitish opacities with unclear borders in the central area of the cornea and limbus, located in the stroma, hence its name. The epithelium appears grayish and defective, often developing erosions. The cornea is reduced in thickness. The condition is caused by a mutation in the Carbohydrate Sulfotransferaze 6 gene—CHST6. Kobayashi *et al.* conducted a CFM examination of two patients with macular dystrophy. They established highly reflective deposits in the basal epithelium, as well as in the anterior and middle sections of the stroma, some being dark striated. Normal keratocytes were not visualized [31] [32] [47].

Schnyder crystalline corneal dystrophy (SCCD) is an autosomal dominant disease. When biomicroscopy is performed, cholesterol deposits are observed in the stroma and Bowman's membrane, with diffuse grayish opacification of the surrounding cornea. The degree of alterations progresses with age from the central to the peripheral part of the cornea, in some cases with unilateral involvement. Thanks to CFM, highly reflective deposits in the form of elongated
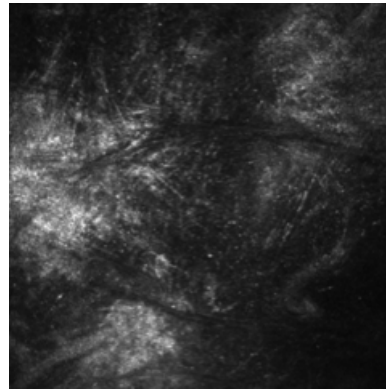
Figure 3. Lattice corneal dystrophy (LCD). *In vivo* confocal microscopy image shows filaments corresponding to lattice lines within the stroma.

crystals are differentiated in the anterior sections of the stroma. Decreased keratocyte density is also observed [50] [51] [52]. Fine crystalline deposits are found in the posterior parts of the stroma, decreasing in brightness and number further deep [51] [53]. Over the course of time, the cornea loses its normal architecture; extensive intra- and extracellular crystalline deposits, as well as the accumulation of extracellular matrix, are observed. This all leads to a loss of corneal transparency and disintegration in the subbasal nerve plexus. Nerve fibers exhibit pronounced tortuosity [32] [50] [52].

Congenital stromal Corneal Dystrophy (CSCD) shows a slow to no progression, and has autosomal dominant inheritance. Through biomicroscopy, opacities in all layers of the stroma and bilaterally in all areas of the cornea could be seen. No vascularization or surface erosions are detected. Pachymetry shows increased corneal thickness. The cells in the epithelial layer manifest no changes in the CFM image. Increased reflectivity is established in the anterior parts of the stroma [31].

Fleck Corneal Dystrophy (FCD) is a rare, autosomal dominant dystrophy with bilateral involvement. Small punctate gray-whitish opacities have been biomicroscopically detected in all layers of the stroma. Between the opacities, spreading from the center towards the periphery, the cornea appears normal. Intracellular hyperreflective punctate deposits of various shape are differentiated in the stroma by CFM. They consist mainly of small spherical materials with a size of 1 - 18 μm, which are sometimes encapsulated in cystic structures with dimensions of 50 - 110 μm in diameter, in the middle and posterior sections of the stroma [32] [54] [55]. Reflective inclusions are detected in the layer of the subbasal nerve plexus, the number and density of nerve fibers being reduced, which contributes to the reduced corneal sensitivity in Fleck dystrophy [56].

Posterior amorphous corneal dystrophy (PACD) is characterized by the presence of grayish-white, sheet-like opacities in all layers of the stroma, with a high concentration in the posterior stroma. The pachymetric map shows corneal thinning of up to below 380 μm, and the topography reveals flattening of the corneal curvature of up to 41D with hypermetropia. Protrusion of Schwalbe's

line, iridocorneal adhesions, corectopia, pseudopolycoria and anterior synechiae have been reported. Erdem *et al.* described a case of PACD in which CFM reveals micro-folds and diffusely distributed sheet-like deposits extracellularly in the posterior stroma, just before the endothelial layer [57].

Central Cloudy Dystrophy of Francois (CCDF) is a bilateral, symmetrical dystrophy. Numerous dense polygonal grayish opacities, occupying the central area of the cornea, resembling crocodile shagreen, are established. Visual acuity is normal. Kobayashi *et al.* reported two cases of CCDF, where small highly reflective granules and deposits in the anterior stroma were differentiated by CFM. No changes were detected in the epithelial layer, the middle sections of the stroma or the endothelial layer, but fine low-reflective striae of highly variable appearance were visualized in the posterior parts of the stroma [32] [58].

Pre-Descemet Corneal Dystrophy (PDCD) usually occurs after the age of 30. Polymorphic opacities (similar to Cornea farinata and Fleck) are biomicroscopically established in the corneal stroma [32]. CFM reveals extra- and intracellular polymorphic hyperreflective inclusions, varying in size, right in front of the Descemet's membrane [59]. It is assumed that intracellular inclusions are actually modified keratocytes, and the small extracellular particles are lysosomes, containing lipofuscin [32] [60].

Endothelial dystrophies

Fuchs' Endothelial Corneal Dystrophy (FECD) is a bilateral slowly progressing corneal dystrophy, which results in dysfunction of the endothelial cell layer. It is clinically manifested with pronounced changes in the endothelial layer – cornea guttata, pigment deposits, thickening of the Descemet's membrane, edema of the stroma and epithelium with bullae, subepithelial fibrosis [32]. A number of rounded hyporeflective zones with a centrally illuminated hyperreflective peak (point) in the endothelial cell layer [61]-[66], as well as pronounced pleomorphism, polymegatism and a reduced number of endothelial cells [31], are visualized on the CFM (Figure 4). Some blurring of the collagen fibrils and a
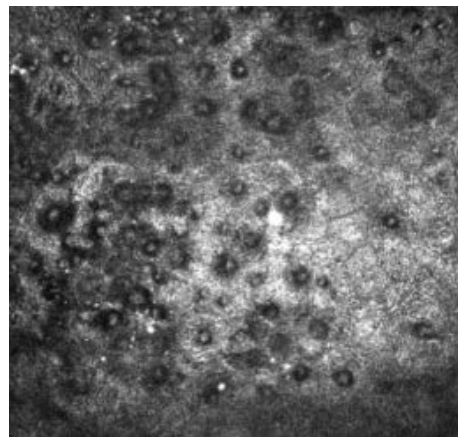

Figure 4. *In vivo* confocal microscopy image of endothelial dystrophy: cornea guttata poly-megathism and pleomorphism of endothelial cells associated with round hyporeflective structures sometimes containing reflective material and corresponding to guttae.

sparse population of keratocytes in the anterior sections [58] were established in the stroma. In all the cases described, a thickening of the Descemet's membrane was detected [67] [68]. A lack of subbasal nerve plexus is also revealed [68].

Grupcheva *et al.* used CFM for differential diagnosis of corneal diseases, occurring with reduced corneal transparency and edema, which demonstrates the ability of CFM to differentiate the presence of guttae in cornea guttata, as well as Fuchs' dystrophy, emphasizing the capabilities of CFM to produce images of endothelial cells in the presence of corneal edema, unlike specular microscopy [69].

Posterior polymorphous corneal dystrophy (PPCD) is frequently taken into consideration with regards to Fuchs' dystrophy, when a differential diagnosis is made. It is often asymmetric. Opacities are detected both in the Descemet's membrane and the endothelial layer: grayish opacities, single or grouped vesicular lesions, grayish-white linear opacities, which may also affect the stroma. Vesicular lesions are visualized on CFM: rounded hyporeflective areas with demarcated single cellular elements in the middle, bearing a resemblance to a "doughnut". There is pronounced polymegatism of the endothelial cells [31].

There are no published data from CFM studies on Congenital hereditary endothelial dystrophy (CHED) or X-linked endothelial corneal dystrophy (XECD).

3.2. Keratitis

Langerhans cells (LCs)

CFM allows *in vivo* imaging and evaluation of Langerhans Cells (LCs) in the human cornea, clarifying their morphology and distribution. LCs are corpuscular particles with projections (dendrites) and a diameter of up to 15 μm. Their distribution increases from the center to the periphery of the cornea. Morphologically there are three types of LCs: with missing dendrites, with small dendrites and such with long dendrites, forming a network.

LCs with long dendritic projections are located in the corneal periphery, whereas in the central parts there are LCs without any projections, which probably accounts for their immaturity. Immature forms are capable of capturing antigens, while mature forms are able to sensitize T-cells, through MHC (Major histocompatibility complex) molecules, thus being part of the immune system [8] [20] [70].

Their density in a healthy subject ranges from 0 - 64 cells/mm^2 (34 ± 3 cells/mm^2) in the central zone, and from 0 - 208 cells/mm^2 (98 ± 8 cells/mm^2) – in the periphery.

Zhivov *et al.* reported a significant increase in the density of LCs when contact lenses are worn: 78 ± 25 cells/mm^2 in the center up to 210 ± 24 cells/mm^2 in the periphery, the gradient of distribution from the center to the periphery being maintained. In the center of the cornea, the density decreases significantly the longer the period of wearing contact lenses is [8] [71].

All of this suggests that LCs are involved in the immune and inflammatory responses, thus determining cell-mediated immunity [20].

Guthoff *et al.* presented a CFM study on patients suffering from corneal inflammatory diseases [8] [20] [72] [73]. Leukocyte infiltration was differentiated as hyperreflective cells in the layer of wing epithelial cells. During an inflammatory process, the mature forms of LCs predominate, localized in the layer of basal epithelial cells.

Bacterial keratitis

Corneal infiltrates are identified as massive leukocyte infiltration at the level of wing and basal epithelial cells (**Figure 5**), while in corneal ulcers, in addition to the tissue lesion, there is edema of the surrounding tissue and infiltration of leukocytes and mature Langerhans cells [73] (**Figure 6**).

Viral keratitis

Viral keratitis can be easily and accurately diagnosed with CFM. A so-called "wire network" is detected, consisting of nerve fibers from the subepithelial nerve plexus and dendritic cells [8] [20] [72] [74]. A reduction in the number of LCs is a clinical sign of recovery of the cornea from the viral infection (**Figure 7**)

In their study on patients with unilateral HSV and HZV involvement, Hamrah *et al.* reported a significant decrease in the number of superficial epithelial cells in eyes with severely reduced corneal sensitivity. The cells are also larger in size. An increased number of desquamated epithelial cells was reported too. All these finds correlated strongly with a reduction in both the total length of nerve fibers and the corneal sensitivity [75] [76].

Muller *et al.* established a significant decrease in the density of endothelial cells, correlating with the reduced total length of nerve fibers in both eyes of patients with unilateral HSV keratitis involvement [77].
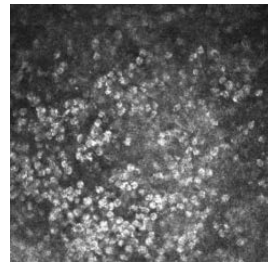

Figure 5. *In vivo* confocal microscopy image of corneal infiltrates – multiple cellular abnormalities at the ulcer edges: hyperreflective cells (leukocytes), reflective nuclei and polymorphism.
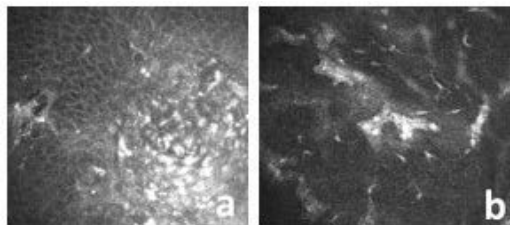

Figure 6. Corneal wound healing: (a) activated corneal epithelium with reflective cells; (b) stroma- numerous activated keratocytes in the anterior stroma, fibrosis and dendritic cells.
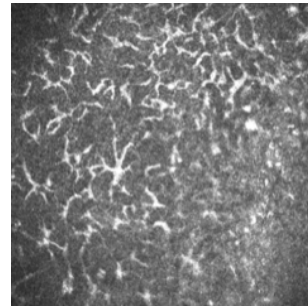
Figure 7. Viral keratitis: herpetic keratitis—typical wire netting (level of subepithelial nerve plexus infiltrated with dendritic cells).

Acanthamoeba keratitis

Acanthamoeba keratitis often remains undiagnosed due to non-specific clinical manifestations. Microbiological tests require time, leading to delays in specific treatment and frequent complications. The fast and reliable identification of Acanthamoeba is one of the most valuable applications of CFM in clinical practice. The differentiation of cysts and trophozoites secures a quick diagnosis and timely treatment [8] [78] [79] [80] [81] [82].

The first identification of Acanthamoeba with CFM was reported in 1992 [83], and shortly thereafter the American Academy of Ophthalmology adopted CFM as an accompanying diagnostic method [84].

The cystic form is characterized by a double wall, hyperreflective structure, a spherical or ovoid shape with dimensions of 15 - 28 μm in diameter in the epithelium and stroma (**Figure 8(a)** and **Figure 8(b)**). The double wall is not always visible, which complicates the differentiation from leukocytes or epithelial cell nuclei. Trophozoites are 25 - 40 μm in diameter, having a hyperreflective structure and ovoid shape [85].

Numerous different clinical studies attribute 80% - 100% reliability to the CFM diagnostic data on Acanthamoeba, while the data from slit-lamp biomicroscopy have been found unconvincing [12] [85].

Mycotic keratitis

Mycotic keratitis is a primary cause of blindness, especially in the tropics. It often remains undiagnosed due to the high variability of the clinical finds. There is often poor susceptibility to treatment, leading to the development of endophthalmitis and blindness.

The diagnostic gold standard is microbiological testing, but it is time-consuming and the cultures frequently remain negative.

CFM provides quick and accurate diagnostics by imaging the hyphae and filaments with high reliability – 78% - 94%, according to various studies [8] [85].

Aspergillus hyphae are hyperreflective and have dichotomous branches below 45˚ with dimensions of 5 - 10 μm in diameter [86]. Conversely, *Fusarium* demonstrates branches below 90˚. *Paecilomyces* show varying thin branches, forming rings [87]. The hyperreflective structures must be differentiated from nerve fibers, which have a more regular architecture, those in the stroma having
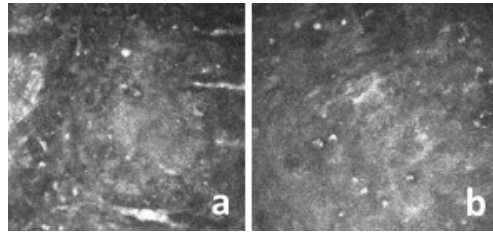
Figure 8. Acanthamoeba keratitis- corneal microcysts (cystic stages of life cycle, round and up to 10 with double wall) are visible at the level of the deeper basal cells an the anterior stroma ((a), (b)).

a larger diameter (25 - 50 μm). The filaments are 200 - 400 μm in length. *Candida albicans* have round embossed bodies measuring 10 - 40 μm in length and 5 - 10 μm in width [88]. *Candida parapsilosis*, in contrast, figures as a small hyperreflective rounded structure of 3 - 5 μm [87].

3.3. Dry Eye

Dry eye syndrome is one of the most common diseases in ophthalmology. It is characterized not only by disorders in the tear film but also by a violation of homeostasis and the structure of the anterior ocular surface.

With its capabilities, CFM allows us to see changes in the corneal epithelium, immune and inflammatory cells, nerve fibers, keratocytes and Meibomian glands at a structural level.

The alterations in the epithelial layer are characterized by decreased superficial cell density and increased basal cell density [89] [90] [91] [92].

In the layer of superficial epithelium, some variations in size are detected, as well as an increased number of hyperreflective cells (probably desquamable) with clearly demarcated nuclei [8].

During the more advanced stages of the disease, alterations in the deeper layers of the cornea are reported too. In the basal epithelial layer, there is an increased number of LCs in the central and peripheral cornea. The amount reported does not determine the severity of the disease, but can be used to monitor treatment [8] [93] [94] [95].

The stroma shows the presence of hyperreflective keratocytes, called by some authors "activated", interpreted as metabolically activated by inflammatory mediators [85] [90].

The nerve fibers of the subbasal nerve plexus demonstrate a pronounced tortuosity with a granular structure of the fibers and abnormal branches [85].

In their study, Castillo *et al.* reported decreased nerve fiber density in the subbasal nerve plexus [96].

Kheirkhah *et al.* conducted a study on 45 patients (90 eyes) with moderate to severe dry syndrome, using CFM to examine the density of endothelial cells, subbasal nerve fibers and dendritic cells. The control group comprised 15 healthy patients (30 eyes), of corresponding age and sex. The results demonstrated a significant decrease in endothelial cells and subbasal nerve fibers, as well as a sig-

nificant increase in dendritic cells in the dry syndrome group, compared to the control group [97].

CFM can also provide imaging and evaluation of the Meibomian glands. A qualitative study of the structure is performed – diameter, density, diameter of the orifice, as well as the periglandular density of the inflammatory cells [97] [98] [99] [100].

Furthermore, the method permits a semi-quantitative assessment of the glandular secretion, taking into account the reflectivity, as well as the structure of the duct wall [99] [100] [101].

When there is a dysfunction of the Meibomian glands, their size is increased but the density is decreased, hyperreflective secretion being found in the ducts. In the case of dry eye syndrome, the Meibomian glands are reduced in volume, the inflammatory cells demonstrate an increased density, and the periglandular tissue is homogeneous [85].

A number of CFM studies have been conducted on the conjunctiva of patients suffering from dry syndrome. Hong *et al.* [102] established the formation of epithelial cysts, as well as a reduced density of conjunctival epithelial cells and goblet cells.

In CFM images, goblet cells figure as oval hyperreflective cells of large size and relatively homogeneous brightness. The density of goblet cells on CFM is 332 ± 137 cells/ mm^2 compared to impression cytology, where the reported density is 200 ± 141 cells/mm^2 in patients with Sjogren's syndrome, a significantly positive correlation being established [101].

Wakamatsu *et al.* [103] reported that patients with Sjogren's syndrome demonstrated a reduced density of conjunctival epithelial cells, in comparison to the group of healthy individuals. The same find was established in patients with dry syndrome. The group of patients with Sjogren's syndrome showed a significant increase in the density of conjunctival epithelial microcysts, compared to the group of healthy individuals, while the dry syndrome group demonstrated no significant difference.

The mean density of inflammatory cells was significantly increased in the Sjogren's syndrome group (433 ± 435.8 cells/mm^2) and in the dry syndrome group (134.8 ± 124.2 cells/mm^2), unlike the control group of healthy eyes (10 ± 17.9 cells/mm^2) [101] [101].

The CFM studies performed on patients with dry eye syndrome reveal a decrease in goblet cell density and an increase in the density of inflammatory cells [101].

3.4. Contact Lenses

CFM considerably contributes to our understanding of the processes occurring in the anterior ocular surface when contact lenses are worn, at a cellular level. In contrast, there was no such possibility to produce an image of a live eye in the past.

There have been several clinical trials with CFM performed by different au-

thors on patients wearing contact lenses [103]-[109]. In the epithelial layer, a larger size of the cells has been established, especially in cases where hard contact lenses are worn. During the process of normal epithelial desquamation, the lenses with high oxygen permeability have the smallest impact [85] [110]. An increased number of LCs has also been reported, in both the center and the periphery of the cornea, within the layer of subbasal nerve plexus. This suggests that the prolonged use of contact lenses may lead to a change in the immune status of the cornea [111].

A number of studies have ascertained a loss of keratocytes with the prolonged use of contact lenses, although there is disagreement about the extent of this effect. Mechanical irritation of the ocular surface results in the subsequent release of inflammatory mediators, which can lead to keratocyte apoptosis [104] [105] [112]-[118].

Corneal sensitivity is also affected by the long-term use of lenses. CFM visualizes the reduction and distribution of nerve fibers, leading to a reduced corneal sensitivity [103] [104].

Chronic morphological changes are also found in the endothelial cell layer, in response to chronic irritation from the prolonged use of contact lenses, increased polymegathism of the cells being reported too [119].

3.5. Corneal Surgery

In addition to diagnostics and monitoring of the anterior segment diseases, CFM gives us the opportunity to evaluate, monitor, and observe the correlation between the morphological and functional processes which take place in the cornea at a microstructural level, after a surgery has been performed. CFM reveals that the structure and architecture of corneal innervation is not static but dynamic. The recovery process of the nerve fibers is dependent on many factors, such as post-operative period, age, diagnosis and the surgical procedure itself.

Corneal transplantation

After Penetrating Keratoplasty (PK), severely reduced innervation is observed due to the nerve fibers being cut at all levels both in the donor and the recipient corneas. The reinnervation process is slow, and the structure of the nerve fibers is abnormal. After being monitored for more than 3 years, none of the patients showed a full morphological and functional recovery of the corneal innervation. It has been established that the reinnervation of the central cornea with subbasal nerve fibers takes approximately two years, and the stromal nerve fibers about seven months postoperatively [120].

Lamellar keratoplasty has gained wide popularity over the last decade in the treatment of diseases engaging the anterior and posterior corneal surface. Although there is no rupture of nerve fibers from the subbasal nerve plexus, except for the area of incision, there are significant changes in the subbasal and stromal nerve fibers before and after endothelial Keratoplasty (EK) has been performed on patients with Fuchs' dystrophy. The stromal nerve fibers have a pronounced tortuosity and are closely connected with the keratocytes, which suggests an in-

teraction between them. The subbasal nerve fibers show an abnormal structure and a reduced number, which is also associated with decreased corneal sensitivity [85] [121].

Refractive surgery

Laser in situ Keratomileusis (LASIK) and Photorefractive Keratectomy (PRK) are the most widely used refractive corneal procedures. In both types of surgery, corneal tissue is removed through excimer photoablation, a flap being formed on the corneal surface with LASIK.

In PRK, subbasal nerve fibers cannot be identified in the treated area. Full recovery of the nerve fiber density in this area is reported after about 2 years [122], and morphological changes are detected after more than 5 years postoperatively [113] [115]. Despite the anatomical structural changes, which are visualized with CFM, the recovery of corneal sensitivity begins to be clinically evident 4 - 6 weeks after the procedure, complete recovery being achieved after 6 - 12 months [123] [124] [125].

In the first month after LASIK has been performed, a 90% decrease in the density of subbasal and stromal nerve fibers is observed, compared to the preoperative period [126]. A number of studies have ascertained that after the first 6 months, reinnervation in the center of the cornea is visualized [127], and complete regeneration is achieved within 2 - 5 years, according to various authors, after the procedure [122] [128].

A correlation is found between corneal sensitivity, the morphology and density of the nerve fibers in the postoperative period [128] [129] [130].

A study comparing corneal healing and reinnervation, conducted by Sonigo *et al*., reported that no difference could be found between the flap made by a Femto Laser and that made by a mechanical microkeratome [131].

Corneal sensitivity after Laser-Assisted Sub-Epithelial Keratectomy (LASEK) is fully restored 3 months after the procedure, although the density of nerve fibers in the subbasal nerve plexus is decreased by half, 6 months after the procedure Darwish *et al.* [132] reported in their study.

Lee *et al.* also reported significantly reduced nerve fiber density after LASEK and incomplete recovery after a 6-month postoperative period [127].

With both LASIK and PRK, a reduced density of keratocytes was observed over a 5-year postoperative period [133] [134].

Small Incision Lenticule Extraction (SMILE) is an innovative method of correcting refractive errors, where through a minimal incision, an intrastromal lenticle previously formed by a Femto Laser is removed. The method has become widespread in ophthalmic surgery due to its high efficiency, minimal invasiveness, safety and predictability [135] [136] [137] [138]. The minimal invasiveness of the method implies a minimal reduction in the density of nerve fibers. Meiyan *et al.* [135] reported in their study that SMILE causes a considerably less reduced density of nerve fibers in the subbasal nerve plexus 1 week, 1 month and 3 months after the procedure, in comparison to Femto LASIK, density being in correlation with corneal sensitivity.

Corneal Collagen Cross-linking (CXL) and Keratoconus

CFM applied to corneas with keratoconus reveals changes in all the layers of the cornea. Elongated superficial epithelial cells and enlarged basal epithelial cells are visualized. The significant decrease in the density of basal epithelial cells and keratocytes corresponds to the severity of the disease. Vogt's striae are depicted as hyporeflective lines in the stroma. There is also marked polymorphism and polymegatism, as well as significantly reduced ECD. In the layer of the sub-basal nerve plexus, an abnormal architecture and reduced density of nerve fibers are visualized [139].

CXL is a minimally invasive surgical procedure aimed at strengthening the tissue in corneal ectasia and stopping the progression of keratoconus [140] [141] [142].

The action of CLX is based on a photochemical reaction between Riboflavin (Vit B 12) and Ultraviolet rays (UVA).

The processes and effect after the application of CXL at a microstructural level can be visualized with CFM.

Saler and Hafezi *et al.* first reported the identification of a line of demarcation in the corneal stroma, visible two weeks after CXL at a depth of 300 μm, separating the treated anterior stroma from the untreated posterior stroma. They reached the conclusion that the presence of the demarcation line is a direct clinical sign to track efficiency in depth after the performance of CXL [140] [143].

Mazzotta *et al.* detected a transient edematous zone with low keratocyte density, a reflective zone and a deeper zone with mild edema and normal keratocyte population at an approximate depth of 320 μm [140] [144].

Kymionis *et al.* demonstrated the so-called "acellular zone", in which they established the absence of subepithelial nerve plexus and keratocytes up to 300 μm depth, with CFM, one month after CXL [145].

Confocal microscopy of Filtering Blebs (FB) after trabeculectomy

CFM allows visualization of microcysts in the epithelial layer of the conjunctiva (**Figures 9(a)-(c)**), subepithelial tissue (**Figures 10(a)-(d)**), blood vessels (**Figure 11**) and the presence of inflammatory cells in FB tissues [85] [146] [147] [148] [149]. Messmer *et al.* [148] reported a significant correlation between the studied parameters and the function of blebs. Filtering blebs with optically empty epithelial microcysts, stroma with extensive non-encapsulated hyporeflective zones, low degrees of vascularization and tortuosity all correlate with good function.
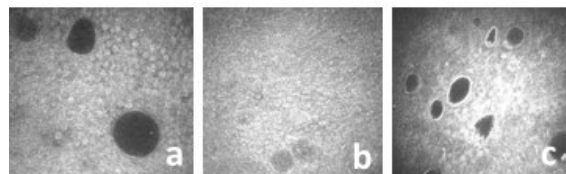

Figure 9. *In vivo* confocal microscopy image shows microcysts in the epithelial layer of the conjunctiva of blebs wall-(a) optically empty; (b) few and filledwith amorphous material, (c) encapsulated epithelial microcysts.
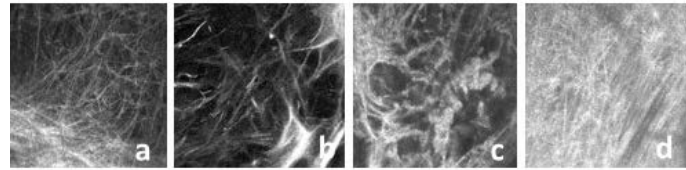
Figure 10. *In vivo* confocal microscopy image shows subepithelial tissue of filtering bleb: (a) loose colagen meshwork; (b) rarified colagen meshwork; (c) hyperreflective stroma; (d) blurred stroma.
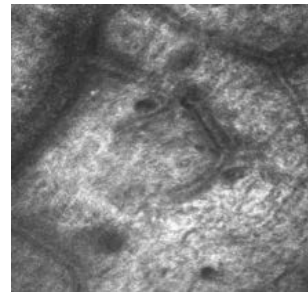

Figure 11. *In vivo* confocal microscopy image shows tortuosity of stromal vessels.

In functioning blebs, normal epithelium is established; loose hyporeflective subepithelial tissue with numerous optically empty spaces is detected too. In non-functioning blebs, an absence or a reduced number of epithelial microcysts, dense hyperreflective subepithelial tissue and a large number of blood vessels are found [146] [147]. Caglar *et al.* reported a significant correlation between the morphological CFM appearance of FB and the function of FB. The presence of epithelial microcysts, capsule-free stromal cysts, minimal vascularization and decreased vascular tortuosity are associated with good FB function, and conversely, hyperreflective dense stroma is associated with poor FB function [150].

4. Conclusion

In vivo confocal microscopy is a relatively new method, which provides detailed information about ocular structures at a cellular level. *In vivo* laser scanning confocal microscopy is a non-invasive examination, allowing layer-by-layer high-resolution imaging at a microstructural level of the tissues of the central and peripheral cornea, eyelid and bulb conjunctiva, eyelids and tear film. It reveals new possibilities to clinicians for evaluation and better understanding of the processes taking place in the structures of the normal anterior ocular surface in abnormal states, as well as after anterior eye segment surgery.

Conflicts of Interest

The authors declare no conflicts of interest regarding the publication of this paper.

References

[1] Guthoff, R.F. and Stave, J. (2006) *In Vivo* Micromorphology of the Cornea: Confoc-

al Microscopy. Principles and Clinical Applications. In: Reinhard, T. and Larkin, F., Eds., *Cornea and External Eye Diseases*, Springer, Berlin, Heidelberg, 173-208. https://doi.org/10.1007/3-540-31226-9_13

[2] Mathers, W.D., Petroll, W.M., Jester, J.V. and Cavanagh, H.D. (1995) Basic Science and Applications of *in Vivo* Microscopy. *Current Opinion in Ophthalmology*, **6**, 86-94. https://doi.org/10.1097/00055735-199508000-00015

[3] Cavanagh, H.D., Jester, J.V., Essepian, J., *et al.* (1990) Confocal Micros-Copy of the Living Eye. *The CLAO Journal*, **16**, 65-73.

[4] Petroll, W.M., Jester, J.V. and Cavanagh, H.D. (1996) *In Vivo* Confocal Imaging. *International Journal of Experimental Pathology*, **36**, 93-129.

[5] Cavanagh, H.D., El-Agha, M.S., Petroll, W.M. and Jester, J.V. (2000) Specular Microscopy, Confocal Microscopy, and Ultrasound Biomicroscopy: Diagnostic Tools of the Past Quarter Century. *Cornea*, **19**, 712-722. https://doi.org/10.1097/00003226-200009000-00016

[6] Mastropasqua, L. and Nubile, M. (2002) Confocal Microscopy of the Cornea. Slack Inc., Thorofare, NJ.

[7] Jalbert, I., Stapleton, F., Papas, E., *et al.* (2003) *In Vivo* Confocal Microscopy of the Human Cornea. *British Journal of Ophthalmology*, **87**, 225-236.

[8] Zhivov, A., Stachs, O., Kraak, R., Stave, J. and Guthoff, R.F. (2006) *In Vivo* Confocal Microscopy of the Ocular Surface. *The Ocular Surface*, **4**, 81-93. https://doi.org/10.1016/S1542-0124(12)70030-7

[9] Paddock, S.W. (2000) Principles and Practices of Laser Scanning Confocal Microscopy. *Molecular Biotechnology*, **16**, 127-149. https://doi.org/10.1385/MB:16:2:127

[10] Minsky, M. (1988) Memoir on Inventing the Confocal Scanning Microscope. *Scanning*, **10**, 128-138. https://doi.org/10.1002/sca.4950100403

[11] White, J.G., Amos, W.B., Durbin, R. and Fordham, M. (1990) Development of a Confocal Imaging System for Biological Epifluorescence Application. In: *Optical Microscopy For Biology*, Wiley-Liss, New York, 1-18.

[12] Kymionis, G.D., Diakonis, V.F., Shehadeh, M.M., Pallikaris, A.I. and Pallikaris, I.G. (2015) Anterior Segment Applications of *in Vivo* Confocal Microscopy. *Seminar in Ophthalmology*, **30**, 243-251. https://doi.org/10.3109/08820538.2013.839817

[13] Masters, B.R. and Thaer, A.A. (1994) Real-Time Scanning Slit Confocal Microscopy of the *in Vivo* Human Cornea. *Applied Optics*, **33**, 695-701. https://doi.org/10.1364/AO.33.000695

[14] You, J.Y. and Botelho, P.J. (2016) Corneal *in Vivo* Confocal Microscopy: Clinical Applications. *Rhode Island Medical Journal*, **99**, 30-33.

[15] Cavanagh, H., Jester, J., Essepian, J., Shields, W. and Lemp, M. (1990) Confocal Microscopy in Living Eye. *CLAO*, **16**, 65-73.

[16] Niederer, R. and McGhee, C. (2010) Clinical *in Vivo* Confocal Microscopy of the Human Cornea in Health and Disease. *Progress in Retinal and Eye Research*, **29**, 30-58. https://doi.org/10.1016/j.preteyeres.2009.11.001

[17] Böhnke, M. and Masters, B.R. (1999) Confocal Microscopy of the Cornea. *Progress in Retinal and Eye Research*, **18**, 553-628. https://doi.org/10.1016/S1350-9462(98)00028-7

[18] Patel, D.V. and McGhee, C.N. (2005) Mapping of the Normal Human Corneal Sub-Basal Nerve Plexus by *in Vivo* Laser Scanning Confocal Microscopy. *Investigative Ophthalmology & Visual Science*, **46**, 4485-4488. https://doi.org/10.1167/iovs.05-0794

[19] Steve, J., Zinser, G., Grümmer, G. and Guthoff, R. (2002) Der modifizierte Heidelberg-Retina-Tomograph HRT Erste Ergebnisse einer *In-vivo*-Darstellung von kornealen Strukturen. *Der Ophthalmologe*, **99**, 276-280.
https://doi.org/10.1007/s003470100535

[20] Kobayashi, A., Yoshita, T. and Sugiyama, K. (2005) *In Vivo* Findings of the Bulbar/Palpebral Conjunctiva and Presumed Meibomian Glands by Laser Scanning Confocal Microscopy. *Cornea*, **24**, 985-988.
https://doi.org/10.1097/01.ico.0000160976.88824.2b

[21] Tavakoli, M., Hossain, P. and Malik, R. (2008) Clinical Applications of Corneal Confocal Microscopy. *Clinical Ophthalmology*, **2**, 435-445.
https://doi.org/10.2147/OPTH.S1490

[22] Guthoff, R.F., Baudouin, C. and Stave, J. (2006) Atlas of Confocal Laser Scanning *In-Vivo* Microscopy in Ophthalmology. Springer, Berlin, Heidelberg, New York.
https://doi.org/10.1007/3-540-32707-X

[23] Eckard, A., Stave, J. and Guthoff, R.E. (2006) *In Vivo* Investigations of the Corneal Epithelium with the Confocal Rostock Laser Scanning Microscope (RLSM). *Cornea*, **25**, 127-131. https://doi.org/10.1097/01.ico.0000170694.90455.f7

[24] Mustonen, R.K., McDonald, M.B., Srivannaboon, S., *et al*. (1998) Normal Human Corneal Cell Populations Evaluated by *in Vivo* Scanning Slit Confocal Microscopy. *Cornea*, **17**, 485-492. https://doi.org/10.1097/00003226-199809000-00005

[25] Popper, M., Morgado, A.M., Qudrado, M.J. and Van Best, M.J. (2004) Corneal Cell Density Measurement *in Vivo* by Scanning Slit Confocal Microscopy: Method and Validation. *Ophthalmic Research*, **36**, 270-276. https://doi.org/10.1159/000081207

[26] Guthoff, R.F., Wienss, H., Hahnel, C. and Wree, A. (2005) Epithelial Innervation of Human Cornea: A Three-Dimensional Study Using Confocal Laser Scanning Fluorescence Microscopy. *Cornea*, **24**, 608-613.
https://doi.org/10.1097/01.ico.0000154384.05614.8f

[27] Muller, L.J., Marfurt, C.F., Kruse, F. and Tervo, T.M. (2003) Corneal Nerves: Structure, Contents and Function. *Experimental Eye Research*, **76**, 521-542.
https://doi.org/10.1016/S0014-4835(03)00050-2

[28] Muller, L.J., Vrensen, G.F., Pels, L., Cardozo, B.N. and Willekens, B. (1997) Architecture of Human Corneal Nerves. *Investigative Ophthalmology & Visual Science*, **38**, 985-994.

[29] Muller, L.J., Pels, L. and Vrensen, G.F. (1996) Ultrastructural Organization of Human Corneal Nerves. *Investigative Ophthalmology & Visual Science*, **37**, 476-488.

[30] Dua, H.S. and Azuara-Blanco, A. (2000) Limbal Stem Cells of the Corneal Epithelium. *Survey of Ophthalmology*, **44**, 415-425.

[31] Sangwan, V.S. (2001) Limbal Stem Cells in Health and Disease. *Bioscience Reports*, **21**, 385-405. https://doi.org/10.1023/A:1017935624867

[32] Weiss, J.S., Møller, H.U., Aldave, A.J., Seitz, B., Bredrup, C., Kivelä, T., Munier, F.L., Rapuano, C.J., Nischal, K.K., Kim, E.K., Sutphin, J., Busin, M., Labbé, A., Kenyon, K.R., Kinoshita, S. and Lisch, W. (2015) IC3D Classification of Cornea Dystrophies—Edition 2. *Cornea*, **34**, 117-159.
https://doi.org/10.1097/ICO.0000000000000307

[33] Shukla, A.N., Cruzat, A. and Hamrah, P. (2012) Confocal Microscopy of Corneal Dystrophies. *Seminars in Ophthalmology*, **27**, 107-116.
https://doi.org/10.3109/08820538.2012.707276

[34] Dighiero, P., Ellies, P., Grateau, G., *et al*. (1999) Review on Corneal Dystrophies.

Journal Français d' Ophtalmologie, **22**, 226-233.

[35] Pouliquen, Y. (1989) Corneal Dystrophies. *La Revue du Praticien*, **39**, 123-127.

[36] Bozkurt, B. and Irkec, M. (2009) *In Vivo* Laser Confocal Microscopic Findings in Patients with Epithelial Basement Membrane Dystrophy. *European Journal of Ophthalmology*, **19**, 348-354. https://doi.org/10.1177/112067210901900304

[37] Hernandez-Quintela, E., Mayer, F., Dighiero, P., *et al.* (1998) Confocal Microscopy of Cystic Disorders of the Corneal Epithelium. *Ophthalmology*, **105**, 631-636. https://doi.org/10.1016/S0161-6420(98)94016-7

[38] Labbe, A., Nicola, R.D., Dupas, B., Auclin, F. and Baudouin, C. (2006) Epithelial Basement Membrane Dystrophy: Evaluation with HRT II Rostock Cornea Module. *Ophthalmology*, **113**, 1301-1308. https://doi.org/10.1016/j.ophtha.2006.03.050

[39] Rosenberg, M.E., Tervo, T.M., Petroll, W.M. and Vesaluoma, M.H. (2000) *In Vivo* Confocal Microscopy of Patients with Corneal Recurrent Erosion Syndrome or Epithelial Basement Membrane Dystrophy. *Ophthalmology*, **107**, 565-573. https://doi.org/10.1016/S0161-6420(99)00086-X

[40] Javadi, M.A., Rezaei-Kanavi, M., Javadi, A. and Nagshshgar, N. (2010) Meesmann Corneal Dystrophy; A Clinico-Pathologic, Ultrastructural and Confocal Scan Report. *Journal of Ophthalmic and Vision Research*, **5**, 122-126.

[41] Patel, D.V., Grupcheva, C.N. and McGhee, C.N. (2005) Imaging the Microstructural Abnormalities of Meesmann Corneal Dystrophy by *in Vivo* Confocal Microscopy. *Cornea*, **24**, 669-673. https://doi.org/10.1097/01.ico.0000154389.51125.70

[42] Tuft, S. and Bron, A.J. (2006) Imaging the Microstructural Abnormalities of Meesmann Corneal Dystrophy by *in Vivo* Confocal Microscopy. *Cornea*, **25**, 868. https://doi.org/10.1097/01.ico.0000251346.00439.a8

[43] Kobayashi, A., Sacurai, M., Shirao, Y., *et al.* (2003) *In Vivo* Confocal Microscopy and Genotyping of a Family with Thiel-Behnke (Honeycomb) Corneal Dystrophy. *Archives of Ophthalmology*, **121**, 1498-1499. https://doi.org/10.1001/archopht.121.10.1498

[44] Kobayashi, A. and Sugiyama, K. (2007) *In Vivo* Laser Confocal Microscopy Findings for Bowman's Layer Dystrophies (Thiel-Behnke and Reis-Bücklers Corneal Dystrophies). *Ophthalmology*, **114**, 69-75. https://doi.org/10.1016/j.ophtha.2006.05.076

[45] Werner, L.P., Werner, L., Dighiero, P., *et al.* (1999) Confocal Microscopy in Bowman and Stromal Corneal Dystrophies. *Ophthalmology*, **106**, 1697-1704.

[46] Dalton, K., Schneider, S., Sorbara, L. and Jones, L. (2010) Confocal Microscopy and Optical Coherence Tomography Imaging of Hereditary Granular Dystrophy. *Contact Lens and Anterior Eye*, **33**, 33-40.

[47] Kaufman, S.C., Beuerman, R.W. and Goldberg, D. (1995) A New Form of Primary, Localized, Corneal Amyloidosis: A Case Report with Confocal Microscopy. *Metabolic, Pediatric, and Systemic Ophthalmology*, **18**, 1-4.

[48] Kobayashi, A., Fujiki, K., Fujimaki, T., Murakami, A. and Sugiyama, K. (2007) *In Vivo* Confocal Microscopy Findings of Corneal Dystrophies. *Archives of Ophthalmology*, **125**, 1168-1173. https://doi.org/10.1001/archopht.125.9.1168

[49] Chiou, A.G., Beuerman, R.W., Kaufman, S.C. and Kaufman, H.E. (1999) Confocal Microscopy in Lattice Corneal Dystrophy. *Graefe's Archive for Clinical and Experimental Ophthalmology*, **237**, 697-701. https://doi.org/10.1007/s004170050299

[50] Rosenberg, M.E., Tervo, T.M., Gallar, J., *et al.* (2001) Corneal Morphology and Sensitivity in Lattice Dystrophy Type II (Familial Amyloidosis, Finnish Type). *Investig-*

ative Ophthalmology & Visual Science, **42**, 634-641.

[51] Ciancaglini, M., Carpineto, P., Doronzo, E., Nubile, M., Zuppardi, E. and Mastropasqua, L. (2001) Morphological Evaluation of Schnyder's Central Crystalline Dystrophy by Confocal Microscopy before and after Phototherapeutic Keratectomy. *Journal of Cataract & Refractive Surgery*, **27**, 1892-1895.
https://doi.org/10.1016/S0886-3350(00)00840-3

[52] Jing, Y. and Wang, L. (2009) Morphological Evaluation of Schnyder's Crystalline Corneal Dystrophy by Laser Scanning Confocal Microscopy and Fourier-Domain Optical Coherence Tomography. *Clinical & Experimental Ophthalmology*, **37**, 308-312. https://doi.org/10.1111/j.1442-9071.2009.02021.x

[53] Vesaluoma, M.H., Linna, T.U., Sankila, E.M., Weiss, S.J. and Tervo, T.M. (1999) *In Vivo* Confocal Microscopy of a Family with Schnyder's Crystalline Corneal Dystrophy. *Ophthalmology*, **106**, 944-951.
https://doi.org/10.1016/S0161-6420(99)00514-X

[54] Jing, Y., Liu, C., Xu, J. and Wang, L. (2009) A Novel UBIAD1 Mutation Identified in Chinese Family with Schnyder Crystalline Corneal Dystrophy. *Molecular Vision*, **15**, 1463-1469.

[55] Pan, F., Yao, Y.F., Nie, X. and Zhang, B. (2011) Clinical Characteristic and *in Vivo* Confocal Microscopic Imaging of Fleck Corneal Dystrophy. *Journal of Zhejiang University. Medical Sciences*, **40**, 321-326.

[56] Grupcheva, C.N., Malik, T.Y., Craig, J.P., Scherwin, T. and McGhee, C.N. (2001) Microstructural Assessment of Rare Corneal Dystrophies Using Real-Time *in Vivo* Confocal Microscopy. *Clinical & Experimental Ophthalmology*, **29**, 281-285.
https://doi.org/10.1046/j.1442-9071.2001.00434.x

[57] Frueh, B.E. and Bohnke, M. (1999) *In Vivo* Confocal Microscopy of Fleck Dystrophy. *Cornea*, **18**, 658-660. https://doi.org/10.1097/00003226-199911000-00005

[58] Erdem, U., Muftuoglu, O. and Hurmeric, V. (2007) *In Vivo* Confocal Microscopy Findings in a Patient with Posterior Amorphous Corneal Dystrophy. *Clinical & Experimental Ophthalmology*, **35**, 99-102.
https://doi.org/10.1111/j.1442-9071.2007.01426.x

[59] Kobayaschi, A., Sudiyama, K. and Huang, A.J. (2004) *In Vivo* Confocal Microscopy in Patients with Central Cloudy Dystrophy of François. *Archives of Ophthalmology*, **122**, 1676-1679. https://doi.org/10.1001/archopht.122.11.1676

[60] Lanza, M., Borrelli, M., Benusiglio, E. and Rasa, N. (2009) *In Vivo* Confocal Microscopy of an Apparent Deep Stroma Corneal Dystrophy: A Case Report. *Cases Journal*, **2**, Article No. 9317. https://doi.org/10.1186/1757-1626-2-9317

[61] Ye, Y.F., Yao, Y.F., Zhou, P. and Pan, F. (2006) *In Vivo* Confocal Microscopy of Pre-Descemet's Membrane Corneal Dystrophy. *Clinical & Experimental Ophthalmology*, **34**, 614-616. https://doi.org/10.1111/j.1442-9071.2006.01288.x

[62] Yeh, S.I., Liu, T.S., Ho, C.C. and Cheng, H.C. (2011) *In Vivo* Confocal Microscopy of Combined Pre-Descemet Membrane Corneal Dystrophy and Fuchs Endothelial Dystrophy. *Cornea*, **30**, 222-224. https://doi.org/10.1097/ICO.0b013e3181e2cf3f

[63] Chiou, A.G., Kaufman, S.C., Beuerman, R.W., Ohta, T., Soliman, H. and Kaufman, H.E. (1999) Confocal Microscopy in Cornea Guttata and Fuchs' Endothelial Dystrophy. *British Journal of Ophthalmology*, **83**, 185-189.

[64] Kaufman, S.C., Beuerman, R.W. and Kaufman, H.E. (1993) Diagnosis of Advanced Fuchs' Endothelial Dystrophy With the Confocal Microscope. *American Journal of Ophthalmology*, **116**, 652-653. https://doi.org/10.1016/S0002-9394(14)73217-9

[65] Dong, W.L., Zou, L.H., Pan, Z.Q. and Wang, L. (2004) Morphologic Characteristics of Cornea in Fuchs Endothelial Dystrophy Observed by Confocal Microscopy. *Chinese Journal of Ophthalmology*, **40**, 465-470.

[66] Patel, D.V., Phua, Y.S. and McGhee, C.N. (2006) Clinical and Microstructural Analysis of Patients with Hyper-Reflective Corneal Endothelial Nuclei Imaged by *in Vivo* Confocal Microscopy. *Experimental Eye Research*, **82**, 682-687. https://doi.org/10.1016/j.exer.2005.09.006

[67] Hecker, L.A., McLaren, J.W., Bachman, L.A. and Patel, S.V. (2011) Anterior Keratocyte Depletion in Fuchs Endothelial Dystrophy. *Archives of Ophthalmology*, **129**, 555-561. https://doi.org/10.1001/archophthalmol.2010.344

[68] Rokita-Wala, I., Mrukwa-Kominek, E. and Gierek-Ciaciura, S. (2000) Changes in Corneal Structure Observed with Confocal Microscopy during Fuchs Endothelial Dystrophy. *Klinika Oczna*, **102**, 339-344.

[69] Mustonen, R.K., McDonald, M.B., Srivannaboon, S., Tan, A.L., Doubrava, M.W. and Kim, C.K. (1998) *In Vivo* Confocal Microscopy of Fuchs' Endothelial Dystrophy. *Cornea*, **17**, 493-503. https://doi.org/10.1097/00003226-199809000-00006

[70] Grupcheva, C.N., Craig, J.P., Sherwin, T. and McGhee, C.N. (2001) Differential Diagnosis of Corneal Oedema Assisted by *in Vivo* Confocal Microscopy. *Clinical & Experimental Ophthalmology*, **29**, 133-137. https://doi.org/10.1046/j.1442-9071.2001.00393.x

[71] Harman, P., Zhang, Q., Liu, Y. and Dana, M.R. (2002) Novel Characterization of MHC Class II-Negative Population of Resident Corneal Langerhans Cell-Type Dendritic Cells. *Investigative Ophthalmology & Visual Science*, **43**, 639-646.

[72] Zhivov, A., Steave, J., Vollimar, B. and Guhtoff, R.E. (2005) Evaluation of Langerhans Cell Density and Distribution in the Corneal Epithelium of Healthy Volunteers and Contact Lens Wearers With in vivo Confocal Microscopy. *Investigative Ophthalmology & Visual Science*, **46**, 2823.

[73] Guthoff, R.F. and Stave, J. (2006) *In Vivo* Micromorphology of the Cornea: Confocal Microscopy. Principles and Clinical Applications. In: Reinhard, T. and Larkin, F., Eds., *Cornea and External Eye Diseases*, Springer, Berlin, Heidelberg, 173-208. https://doi.org/10.1007/3-540-31226-9_13

[74] Zhivov, A., Steave, J. and Guthoff, R.F. (2005) *In Vivo* konfokale Mikroskopie von Hornhautulzera. *Klinische Monatsblätter für Augenheilkunde*, **222**, KV8. https://doi.org/10.1055/s-2005-871590

[75] Knappe, S., Stave, J. and Guthoff, R.F. (2005) Epidemic Keratoconjunctivitis. *In Vivo* Representation of Corneal Histopathological Structures with the Confocal Rostocker Laser Scanning Microscope (RLSM). *Der Ophthalmologe*, **102**, 798-801. https://doi.org/10.1007/s00347-004-1046-9

[76] Hamrah, P., Sahin, A., Dasttjerdi, M., Shachatit, B., Bayhan, H., Dana, R. and Pavan-Langston, D. (2012) Cellular Changes of the Corneal Epithelium and Stroma in Herpes Simplex Keratitis: An *in Vivo* Confocal Microscopy Study. *Ophthalmology*, **119**, 1791-1797. https://doi.org/10.1016/j.ophtha.2012.03.005

[77] Hamrah, P., Sahin, A., Dasttjerdi, M., Shachatit, B., Bayhan, H., Dana, R. and Pavan-Langston, D. (2015) *In Vivo* Confocal Microscopic Changes of the Corneal Epithelium and Stroma in Patients with Herpes Zoster Ophtalmicus. *American Journal of Ophthalmology*, **159**, 1036-1044. https://doi.org/10.1016/j.ajo.2015.03.003

[78] Muller, R., Poumirzaie, R., Pavan-Langston, D., Cavalcanti, B., Aggarwal, S., Colon, C., Jamali, A., Cruzat, A. and Hamrah, P. (2015) *In Vivo* Confocal Microscopy Demonstrates Bilateral Loss of Endothelial Cells in Unilateral Herpes Simplex Kerati-

tis. *Investigative Ophthalmology & Visual Science*, **56**, 4899-4906.
https://doi.org/10.1167/iovs.15-16527

[79] Winchester, K., Mathers, W.D., Sutphin, J.E. and Daley, T.E. (1995) Diagnosis of Acanthamoeba Keratitis *in Vivo* with Confocal Microscopy. *Cornea*, **14**, 10-17.
https://doi.org/10.1097/00003226-199501000-00003

[80] Cavanagh, H.D. and McCulley, J.P. (1996) *In Vivo* Confocal Microscopy and Acanthamoeba Keratitis. *American Journal of Ophthalmology*, **121**, 207-208.
https://doi.org/10.1016/S0002-9394(14)70586-0

[81] Pfister, D.R., Cameron, J.D., Krachmer, J.H. and Holland, E.J. (1996) Confocal Microscopy Findings of *Acanthamoeba* Keratitis. *American Journal of Ophthalmology*, **121**, 119-128. https://doi.org/10.1016/S0002-9394(14)70576-8

[82] Cho, B.J. and Holland, E.J. (1998) *In Vivo* Tandem Scanning Confocal Microscopy in Acanthamoeba Keratitis. *Korean Journal of Ophthalmology*, **12**, 112-117.
https://doi.org/10.3341/kjo.1998.12.2.112

[83] Mathers, W.D., Nelson, S.E., Lane, J.L., *et al.* (2000) Confirmation of Confocal Microscopy Diagnosis of Acanthamoeba Keratitis Using Polymerase Chain Reaction Analysis. *Archives of Ophthalmology*, **118**, 178-183.
https://doi.org/10.1001/archopht.118.2.178

[84] Chew, S.J., Feuerman, R.W., Assouline, M., Kaufman, H.E., Barron, B.A. and Hill, J.M. (1992) Early Diagnosis of Infectious Keratitis with *in Vivo* Real Time Confocal Microscopy. *The CLAO Journal*, **18**, 197-201.

[85] Kaufman, S.C., Musch, D.C., Belin, M.W., Cohen, E.J., Meisler, D.M., Reinhart, W.J., *et al.* (2004) Confocal Microscopy: A Report by the American Academy of Ophthalmology. *Ophthalmology*, **111**, 396-406.
https://doi.org/10.1016/j.ophtha.2003.12.002

[86] Villani, E., Baudoin, C., Efron, N., Hamrah, P., Kojima, T., Patel, S., Pflugfelder, S., Zhivov, A. and Dorgu, M. (2014) *In Vivo* Confocal Microscopy of the Ocular Surface: From Bench to Bedside. *Current Eye Research*, **39**, 213-231.
https://doi.org/10.3109/02713683.2013.842592

[87] Kumar, R.L., Cruzat, A. and Hamrah, P. (2010) Current State of *in Vivo* Confocal Microscopy in Management of Microbial Keratitis. *Seminars in Ophthalmology*, **25**, 166-170. https://doi.org/10.3109/08820538.2010.518516

[88] Baniasadi, N., Cruzat, A., Witkin, D., Stacey, R., Jakobiec, F.A., Chodosh, T., *et al.* (2011) *In Vivo* Confocal Microscopy for *Paecilomyces lilacinus* and *Candida parapsilosis* Fungal Keratitis. *Investigative Ophthalmology & Visual Science*, **52**, 5856.

[89] Labbe, A., Khammari, C., Dupas, B., Gabison, E., Brasnu, E., Labetoulle, M., *et al.* (2009) Contribution of *in Vivo* Confocal Microscopy to the Diagnosis and Management of Infectious Keratitis. *The Ocular Surface*, **7**, 41-52.
https://doi.org/10.1016/S1542-0124(12)70291-4

[90] Tuominen, I.S., Konttinen, Y.T., Vesaluoma, M.H., Moilanen, J.A., Helinto, M. and Tervo, T.M. (2003) Corneal Innervation and Morphology in Primary Sjögren's Syndrome. *Investigative Ophthalmology & Visual Science*, **44**, 2545-2549.
https://doi.org/10.1167/iovs.02-1260

[91] Villani, E., Galimberti, D., Viola, F., Mapelli, C. and Ratiglia, R. (2007) The Cornea in Sjögren's Syndrome: An *in Vivo* Confocal Study. *Investigative Ophthalmology & Visual Science*, **48**, 2017-2022. https://doi.org/10.1167/iovs.06-1129

[92] Villani, E., Galimberti, D., Viola, F., Mapelli, C., Del Pappa, N. and Ratiglia, R. (2008) Corneal Involvement in Rheumatoid Arthritis: An *in Vivo* Confocal Study. *Investigative Ophthalmology & Visual Science*, **49**, 560-564.

https://doi.org/10.1167/iovs.07-0893

[93] Zhang, X., Chen, Q., Chen, W., Cui, L., Ma, H. and Lu, F. (2011) Tear Dynamics and Corneal Confocal Microscopy of Subjects with Mild Self-Reported Office Dry Eye. *Ophthalmology*, **118**, 902-907. https://doi.org/10.1016/j.ophtha.2010.08.033

[94] Alhatem, A., Cavalcanti, B. and Hamrah, P. (2012) *In Vivo* Confocal Microscopy in Dry Eye Disease and Related Condition. *Seminars in Ophthalmology*, **27**, 138-148. https://doi.org/10.3109/08820538.2012.711416

[95] Villani, E., Galimberti, D., Del Papa, N., Nucci, P. and Ratiglia, R. (2013) Inflammation in Dry Eye Associated with Rheumatoid Arthritis: Cytokine and *in Vivo* Confocal Microscopy Study. *Innate Immunity*, **19**, 420-427. https://doi.org/10.1177/1753425912471692

[96] Benitez del Castillo, J.M., Wasfy, M.A., Fernandez, C. and Garcia-Sanches, J. (2004) An *in Vivo* Confocal Masked Study on Corneal Epithelium and Subbasal Nerves in Patients with Dry Eye. *Investigative Ophthalmology & Visual Science*, **45**, 30-35. https://doi.org/10.1167/iovs.04-0251

[97] Kheirkhah, A., Saboo, U., Abud, T., Dohlman, T., Arnoldner, M., Hamrah, P. and Dana, R. (2015) Reduced Corneal Endothelial Cell Density in Patients with Dry Eye Disease. *American Journal of Ophthalmology*, **159**, 1022-1026. https://doi.org/10.1016/j.ajo.2015.03.011

[98] Matsumoto, Y., Sato, E.A., Ibrahim, O.M., Dogru, M. and Tsubota, K. (2008) The Application of *in Vivo* Laser Confocal Microscopy of the Diagnosis and Evaluation of Meibomian Gland Dysfunction. *Molecular Vision*, **14**, 1263-1271.

[99] Ibrahim, O.M., Mastumoto, Y., Dogru, M., Adan, E.S., Wakamatsu, T.H., Goto, T., *et al.* (2010) The Efficacy, Sensitivity, and Specificity of *in Vivo* Laser Confocal Microscopy in the Diagnosis of Meibomian Gland Dysfunction. *Ophthalmology*, **117**, 665-672. https://doi.org/10.1016/j.ophtha.2009.12.029

[100] Villani, E., Beretta, S., De Capitani, M., Galimberti, D., Viola, F. and Ratiglia, R. (2011) *In Vivo* Confocal Microscopy of Meibomian Glands in Sjögren's Syndrome. *Investigative Ophthalmology & Visual Science*, **52**, 933-939. https://doi.org/10.1167/iovs.10-5995

[101] Villani, E., Ceresara, G., Beretta, S., Magnani, F., Viola, F. and Ratiglia, R. (2011) *In Vivo* Confocal Microscopy of Meibomian Glands in Contact Lens Wearers. *Investigative Ophthalmology & Visual Science*, **52**, 5215-5219. https://doi.org/10.1167/iovs.11-7427

[102] Hong, J., Zhu, W., Zhuang, H., Xu, J., Sun, X., Le, Q., Li, G. and Wang, Y. (2010) *In Vivo* Confocal Microscopy of Conjunctival Goblet Cells in Patients with Sjögren's Syndrome Dry Eye. *British Journal of Ophthalmology*, **94**, 1454-1458. https://doi.org/10.1136/bjo.2009.161059

[103] Wakamatsu, T.H., Sato, E.A., Matsumoto, Y., Ibrahim, O.M., Dogru, M., Kaido, M., Ishida, R. and Tsubota, K. (2010) Conjunctival *in Vivo* Confocal Scanning Laser Microscopy in Patients with Sjögren's Syndrome. *Investigative Ophthalmology & Visual Science*, **51**, 144-150. https://doi.org/10.1167/iovs.08-2722

[104] Efron, N., Perez-Gomez, I. and Morgan, B.P. (2002) Confocal Microscopic Observations of Stromal Keratocytes during Extended Contact Lens Wear. *Clinical and Experimental Optometry*, **85**, 156-160. https://doi.org/10.1111/j.1444-0938.2002.tb03028.x

[105] Patel, S.V., McLaren, J.W., Hodge, D.O., *et al.* (2002) Confocal Microscopy *in Vivo* in Corneas of Long-Term Contact Lens Wearers. *Investigate Ophthalmology and visual Science*, **43**, 995-1003.

[106] Kallinikos, P., Morgan, P. and Efron, N. (2004) On the Etiology of Keratocyte Loss during Contact Lens Wear. *Investigative Ophthalmology & Visual Science*, **45**, 3011-3020. https://doi.org/10.1167/iovs.04-0129

[107] O'Donell, C. and Efron, N. (2004) Corneal Endothelial Cell Morphometry and Corneal Thickness in Diabetic Contact Lens Wearers. *Optometry and Vision Science*, **81**, 858-862. https://doi.org/10.1097/01.OPX.0000145029.76675.F7

[108] O'Donell, C., Efron, N. and Boulton, A.J. (2001) A Prospective Study of Contact Lens Wear in Diabetes mellitus. *Ophthalmic and Physiological Optics*, **21**, 127-138. https://doi.org/10.1046/j.1475-1313.2001.00555.x

[109] Olivera-Soto, L. and Efron, N. (2003) Morphology of Corneal Nerves in Soft Contact Lens Wear. A Comparative Study Using Confocal Microscopy. *Ophthalmic and Physiological Optics*, **23**, 163-174. https://doi.org/10.1046/j.1475-1313.2003.00106.x

[110] Hollingsworth, J.G. and Efron, N. (2004) Confocal Microscopy of the Corneas of Long-Term Rigid Contact Lens Wearers. *Contact Lens and Anterior Eye*, **27**, 57-64. https://doi.org/10.1016/S1367-0484(04)00018-9

[111] Ladage, P.M., Yamamoto, Y., Ren, D.H., Li, L., Jester, J.V. and Petroll, W.M. (2001) Effects of Rigid and Soft Contact Lens Daily Wear on Corneal Epithelium, Tear Lactate Dehydrogenase, and Bacterial Binding to Exfoliated Epithelial Cells. *Ophthalmology*, **108**, 1279-1288. https://doi.org/10.1016/S0161-6420(01)00639-X

[112] Zhivov, A., Stave, J., Vollmar, B. and Guthoff, R. (2007) *In Vivo* Confocal Microscopic Evaluation of Langerhans Cell Density and Distribution in the Corneal Epithelium of Healthy Volunteers and Contact Lens Wearers. *Cornea*, **26**, 47-54. https://doi.org/10.1097/ICO.0b013e31802e3b55

[113] Bansal, A.K., Mustonen, R.K. and McDonald, M.B. (1997) High Resolution *in Vivo* Confocal Microscopy of the Cornea in Long Term Contact Lens Wear. *Investigative Ophthalmology & Visual Science*, **38**.

[114] Efron, N., Mutalib, H.A., Perez-Gomez, I. and Koh, H.H. (2002) Confocal Microscopic Observations of the Human Cornea Following Overnight Contact Lens Wear. *Clinical and Experimental Optometry*, **85**, 149-155. https://doi.org/10.1111/j.1444-0938.2002.tb03027.x

[115] Jalbert, I. and Stapleton, F. (1999) Effect of Lens Wear on Corneal Stroma: Preliminary Findings. *Australian and New Zealand Journal of Ophthalmology*, **27**, 211-213. https://doi.org/10.1046/j.1440-1606.1999.00205.x

[116] Kallinikos, P., Morgan, P.B. and Efron, N. (2006) Assessment of Stromal Keratocytes and Tear Film Inflammatory Mediators during Extended Wear of Contact Lenses. *Cornea*, **25**, 1-10. https://doi.org/10.1097/01.ico.0000167877.11687.7e

[117] Zhong, X., Chen, X., Xie, R.Z., Yang, J., Li, S., Yang, X., *et al.* (2009) Differences between Overnight and Long-Term Wear of Orthokeratology Contact Lenses in Corneal Contour, Thickness, and Cell Density. *Cornea*, **28**, 271-279. https://doi.org/10.1097/ICO.0b013e318186e620

[118] Yagmur, M., Okay, O., Sizmaz, S., Unal, I. and Yar, K. (2011) *In Vivo* Confocal Microscopy: Corneal Changes of Hydrogel Contact Lens Wearers. *International Ophthalmology*, **31**, 377-383. https://doi.org/10.1007/s10792-011-9466-4

[119] Ohta, K., Shimamura, I., Shiraishi, A. and Ohashi, Y. (2012) Confocal Microscopic Observations of Stromal Keratocytes in Soft and Rigid Contact Lens Wearers. *Cornea*, **31**, 66-73. https://doi.org/10.1097/ICO.0b013e31821b71ff

[120] Nagel, S., Wiegand, W., Thaer, A.A. and Geyer, O.C. (1996) Light Scattering Study of the Cornea in Contact Lens Patients. *In Vivo* Studies Using Confocal Slit Scanning Microscopy. *Der Ophthalmologe*, **93**, 252-256.

[121] Cruzat, A., Pavan-Langston, D. and Hamrah, P. (2010) *In Vivo* Confocal Microscopy of Corneal Nerves: Analysis and Clinical Correlation. *Seminars in Ophthalmology*, **25**, 171-177. https://doi.org/10.3109/08820538.2010.518133

[122] Niederer, R.L., Perumal, D., Sherwin, T. and McGhee, C.N. (2007) Corneal Innervation and Cellular Changes after Corneal Transplantation: An *in Vivo* Confocal Microscopy Study. *Investigative Ophthalmology & Visual Science*, **48**, 621-626. https://doi.org/10.1167/iovs.06-0538

[123] Erie, J.C., McLaren, J.W., Hodge, D.O. and Bourne, W.M. (2005) Recovery of Corneal Subbasal Nerve Density after PRK and LASIK. *American Journal of Ophthalmology*, **140**, 1059-1064. https://doi.org/10.1016/j.ajo.2005.07.027

[124] Linna, T. and Tervo, T. (1997) Real-Time Confocal Microscopic Observations on Human Corneal Nerves and Wound Healing after Excimer Laser Photorefractive Keratectomy. *Current Eye Research*, **16**, 640-649. https://doi.org/10.1076/ceyr.16.7.640.5058

[125] Pérez-Santonja, J.J., Sakla, H.F., Cardona, C., Chipont, E. and Alió, J.L. (1999) Corneal Sensitivity after Photorefractive Keratectomy and Laser *in Situ* Keratomileusis for Low Myopia. *American Journal of Ophthalmology*, **127**, 497-504. https://doi.org/10.1016/S0002-9394(98)00444-9

[126] Kauffmann, T., Bodanowitz, S., Hesse, L. and Kroll, P. (1996) Corneal Reinnervation after Photorefractive Keratectomy and Laser *in Situ* Keratomileusis: An *in Vivo* Study with a Confocal Videomicroscope. *German Journal of Ophthalmology*, **5**, 508-512.

[127] Lee, B.H., McLaren, J.W., Erie, J.C., Hodge, D.O. and Bourne, W.M. (2002) Reinnervation in the Cornea after LASIK. *Investigative Ophthalmology & Visual Science*, **43**, 3660-3664.

[128] Calvillo, M.P., McLaren, J.W., Hodge, D.O. and Bourne, W.M. (2004) Corneal Reinnervation after LASIK: Prospective 3-Year Longitudinal Study. *Investigative Ophthalmology & Visual Science*, **45**, 3991-3996. https://doi.org/10.1167/iovs.04-0561

[129] Perez-Gomez, I. and Efron, N. (2003) Change to Corneal Morphology after Refractive Surgery (Myopic Laser *in Situ* Keratomileusis) as Viewed with a Confocal Microscope. *Optometry and Vision Science*, **80**, 690-697. https://doi.org/10.1097/00006324-200310000-00010

[130] Linna, T.U., Vesaluoma, M.H., Perez-Santonja, J.J., Petroll, W.M., Alió, J.L. and Tervo, T.M. (2000) Effect of Myopic LASIK on Corneal Sensitivity and Morphology of Subbasal Nerves. *Investigative Ophthalmology & Visual Science*, **41**, 393-397.

[131] Sonigo, B., Iordanidou, V., Chong-Sit, D., *et al.* (2006) *In Vivo* Corneal Confocal Microscopy Comparison of Intralase Femtosecond Laser and Mechanical Microkeratome for Laser *in Situ* Keratomileusis. *Investigative Ophthalmology & Visual Science*, **47**, 2803-2811. https://doi.org/10.1167/iovs.05-1207

[132] Darwish, T., Brahma, A., O'Donnell, C. and Efron, N. (2007) Subbasal Nerve Fiber Regeneration after LASIK and LASEK Assessed by Noncontact Esthesiometry and *in Vivo* Confocal Microscopy: Prospective Study. *Journal of Cataract & Refractive Surgery*, **33**, 1515-1521. https://doi.org/10.1016/j.jcrs.2007.05.023

[133] Erie, J.C., Patel, S.V., McLaren, J.W., *et al.* (2006) Corneal Keratocyte Deficits after Photorefractive Keratectomy and Laser *in Situ* Keratomileusis. *American Journal of Ophthalmology*, **141**, 799-809. https://doi.org/10.1016/j.ajo.2005.12.014

[134] Erie, J.C., McLaren, J.W., Hodge, D.O., *et al.* (2005) Long-Term Corneal Keratoctye Deficits after Photorefractive Keratectomy and Laser *in Situ* Keratomileusis. *Trans-*

actions of the American Ophthalmological Society, **103**, 56-66.

[135] Li, M.Y., Niu, L.L., Qin, B., Zhou, Z. M., Ni, K., Le, Q. H., Xiang, J., Wei, A. J., Ma, W. P. and Zhou, X. T. (2013) Confocal Comparison of Corneal Reinnervation after Small Incision Lenticule Extraction (SMILE) and Femtosecond Laser *in Situ* Keratomileusis (FS-LASIK). *PLoS ONE*, **8**, e81435.
https://doi.org/10.1371/journal.pone.0081435

[136] Vestergaard, A., Ivarsen, A., Asp, S. and Hjortdal, J.O. (2012) Femtosecond (FS) Laser Vision Correction Procedure for Moderate to High Myopia: A Prospective Study of ReLEx® Flex and Comparison with a Retrospective Study of FS-Laser *in Situ* Keratomileusis. *Acta Ophthalmologica*, **91**, 355-362.
https://doi.org/10.1111/j.1755-3768.2012.02406.x

[137] Sekundo, W., Kunert, K.S. and Blum, M. (2011) Small Incision Corneal Refractive Surgery Using the Small Incision Lenticule Extraction (SMILE) Procedure for the Correction of Myopia and Myopic Astigmatism: Results of a 6 Month Prospective Study. *British Journal of Ophthalmology*, **95**, 335-339.
https://doi.org/10.1136/bjo.2009.174284

[138] Shah, R., Shah, S. and Sengupta, S. (2011) Results of Small Incision Lenticule Extraction: All-in-One Femtosecond Laser Refractive Surgery. *Journal of Cataract & Refractive Surgery*, **37**, 127-137. https://doi.org/10.1016/j.jcrs.2010.07.033

[139] Bitirgen, G., Ozkagnici, A., Bozkurt, B. and Malik, R. (2015) *In Vivo* Confocal Microscopic Analysis in Patients with Keratoconus. *International Journal of Ophthalmology*, **8**, 534-539.

[140] Kymionis, G., Grentzelos, M., Plaka, A., Tsoulnaras, K., Diakonis, V., Liakopoulos, D., Kankariya, V. and Pallikaris, A. (2014) Correlation of the Corneal Collagen Cross-Linking Demarcation Line Using Confocal Microscopy and Anterior Segment Optical Coherence Tomography in Keratoconic Patients. *American Journal of Ophthalmology*, **157**, 110-115. https://doi.org/10.1016/j.ajo.2013.09.010

[141] Wollensak, G. (2006) Crosslinking Treatment of Progressive Keratoconus: New Hope. *Current Opinion in Ophthalmology*, **17**, 356-360.
https://doi.org/10.1097/01.icu.0000233954.86723.25

[142] Wollensak, G. and Spoerl, T. (2003) Riboflavin/Ultraviolet-A-Induced Collagen Crosslinking for the Treatment of Keratoconus. *American Journal of Ophthalmology*, **135**, 620-627. https://doi.org/10.1016/S0002-9394(02)02220-1

[143] Seiler, T. and Hafezi, F. (2006) Corneal Cross-Linking-Induced Stromal Demarcation Line. *Cornea*, **25**, 1057-1059.
https://doi.org/10.1097/01.ico.0000225720.38748.58

[144] Mazzotta, C., Balestrazzi, A., Traversi, C., *et al*. (2007) Treatment of Progressive Keratoconus by Riboflavin-UVA-Induced Cross-Linking of Corneal Collagen: Ultrastructural Analysis by Heidelberg Retinal Tomograph II *in Vivo* Confocal Microscopy in Humans. *Cornea*, **26**, 390-397.
https://doi.org/10.1097/ICO.0b013e318030df5a

[145] Kymionis, G.D., Diakonis, V.F., Kalyvianaki, M., *et al*. (2009) One-Year Follow-Up of Corneal Confocal Microscopy after Corneal Cross-Linking in Patients with Post Laser *in Situ* Keratosmileusis Ectasia and Keratoconus. *American Journal of Ophthalmology*, **14**, 774-778. https://doi.org/10.1016/j.ajo.2008.11.017

[146] Labbe, A., Dupas, B., Hamard, P. and Baudouin, C. (2005) *In Vivo* Confocal Microscopy Study of Blebs after Filtering Surgery. *Ophthalmology*, **112**, 1979.

[147] Guthoff, R., Klink, T., Schlunck, G. and Grehn, F. (2006) *In Vivo* Confocal Microscopy of Failing and Functioning Filtering Blebs: Results and Clinical Correlations.

Journal of Glaucoma, **15**, 552-558.
https://doi.org/10.1097/01.ijg.0000212295.39034.10

[148] Messmer, E.M., Zapp, D.M., Mackert, M.J., Thiel, M. and Kampik, A. (2006) *In Vivo* Confocal Microscopy of Filtering Blebs after Trabeculectomy. *Archives of Ophthalmology*, **124**, 1095-1103. https://doi.org/10.1001/archopht.124.8.1095

[149] Amar, N., Labbe, A., Hamard, P., Dupas, B. and Baudouin, C. (2008) Filtering Blebs and Aqueous Pathway an Immunocytological and *in Vivo* Confocal Microscopy study. *Ophthalmology*, **115**, 1154-1161.e4. https://doi.org/10.1016/j.ophtha.2007.10.024

[150] Caglar, C., Karpuzoglu, N., Batur, M. and Yasar, T. (2016) *In Vivo* Confocal Microscopy and Biomicroscopy of Filtering Blebs after Trabeculectomy. *Journal of Glaucoma*, **25**, 377-383. https://doi.org/10.1097/IJG.0000000000000377